Paper No. 14

SEMI-ANALYTIC DETERMINATION OF BENDING FREQUENCIES OF PROPELLER AND HELICOPTER ROTORS

V. Giurgiutiu & R.O. Stafford
(Aeronautics Department, Imperial College, London SW7)

SUMMARY

The equations of motion including shear and rotatory inertia are developed for uncoupled lead-lag and flapping vibrations of beams rotating at constant angular velocity in a fixed plane. Separability assumptions lead to an ordinary coupled differential equation in the space variable. In the special case of zero-incidence beams the equations are uncoupled, and a solution is obtained in terms of four independent functions, each a convergent power series. These beam functions are similar to classic normal beam functions, and application of the boundary conditions yields determinants whose roots are the natural frequencies. A transfer matrix formulation is set up in terms of the above beam functions to cope with non-uniform and twisted beams and the restriction of zero-incidence is lifted. The simplicity and speed of this method is demonstrated by application to propeller and helicopter rotor blades, and spoke diagrams and mass balancing are illustrated.

1. INTRODUCTION

A number of methods have been developed for determination of frequencies and mode shapes of rotating beams including centrifugal force {1} (henceforth CF), Coriolis terms and other effects. Of particular utility is the transfer matrix method {2}. Both shear deformation and rotatory inertia effects have been included, and this method has proved successful in helicopter rotor blade design {3}. The well known Holzer method with the Rayleigh-Southwell correction has been employed with some success to turbo-machinery blade design {4}. Because of the way many methods approximate internal and CF forces as well as geometry, practical problems often require a large number of segments or divisions, thus leading to large matrices or extensive computations.

In view of the similarity of rotating beams to classic continuous beam dynamics, it appears that some advantage accrues if beam functions are developed which represent exactly CF and the Timoshenko corrections. In Section 2 the equations of motion are reviewed, and in Section 3 assumptions are introduced which lead to uncoupled lead-lag and flapping motion. The assumption of steady harmonic response leads to ordinary differential equations, and in Section 4 the Frobenius method is applied and recursion formulae are developed. Elementary, albeit lengthy algebra reduces the general power series fo four explicit polynomials multiplied by four constants determined from the boundary conditions. These polynomials are treated like any known function, and for non-rotating beams they reduce to trigonometric and hyperbolic sine and cosine.

These may be thought of as "beam functions" for rotating beams with shear and rotatory inertia corrections, and they are sufficient for frequency and mode shape analysis. A transfer matrix is defined in Section 5 which allows one to readily formulate problems involving discontinuous and twisted beams. Application of the boundary conditions leads to a determinant (at most 4 x 4) whose roots are the frequencies, and examples in Section 7 include spoke diagrams typical of current helicopters. Because of its simplicity and speed, other parameter studies are feasible and some surprising effects of mass balancing are demonstrated.

2. THE EQUATIONS OF MOTION

Attention is restricted to a uniform beam rotating at constant angular velocity about a stationary axis as shown in Fig. 1. The x-axis is the axis of elastic centres (zero pre-cone), and the principal (η,ζ) axes of the cross-

section are located at incidence angle β measured from the plane of rotation (x,y). The centres of shear and mass are assumed to coincide.

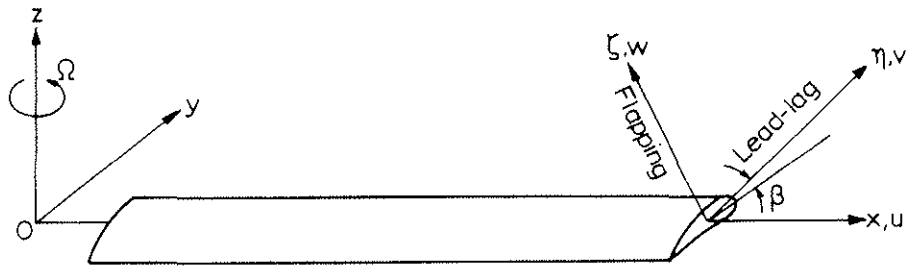

FIG.1: Orientation and motion of a rotating uniform beam.

The usual assumptions of Euler beam theory are invoked. However, the first order corrections (shear and rotatory inertia) to the Engineers Theory of Bending (henceforth ETB) are included. Since most propellers and rotor blades are very stiff in lead-lag compared to flapping, the practical significance of these corrections is probably restricted to the former. The sign convention for moments and shears is shown in Fig. 2.

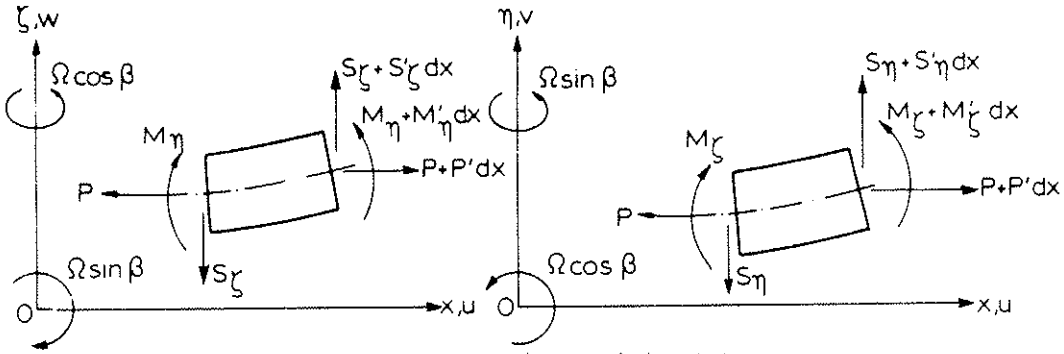

FIG.2: Differential elements for flapping and lead-lag.

After deformation an element of volume $dx\,d\eta\,d\zeta$ initially at position (x,η,ζ) will be, to first order, at $(x+U-\eta V_b'-\zeta W_b',\ V+\eta,\ W+\zeta)$, and the acceleration components are:

$$a_x = \ddot{U} - \eta\ddot{V}_b' - \zeta\ddot{W}_b' - 2\Omega(\dot{V}\cos\beta - \dot{W}\sin\beta) - \Omega^2(x+U-\eta V_b'-\zeta W_b')$$

$$a_y = \ddot{V} + 2(\dot{U} - \eta\dot{V}_b' - \zeta\dot{W}_b')\Omega\cos\beta - \left[(V+\eta)\cos\beta - (W+\zeta)\sin\beta\right]\Omega^2\cos\beta$$

$$a_\zeta = \ddot{W} - 2(\dot{U} - \eta\dot{V}_b' - \zeta\dot{W}_b')\Omega\sin\beta + \left[(V+\eta)\cos\beta - (W+\zeta)\sin\beta\right]\Omega^2\sin\beta$$

By integrating over the element the usual expressions for strain and acceleration, the complete linear coupled equations of motion become [5,6]

$$P' = m\ddot{U} - 2m\Omega(\dot{V}\cos\beta - \dot{W}\sin\beta) - \Omega^2 m(x+U) \qquad (1)$$

$$S_\eta' = m\ddot{V} + 2m\Omega\dot{U}\cos\beta - m\Omega^2(V\cos^2\beta - W\sin\beta\cos\beta) \qquad (2a)$$

$$S_\zeta' = m\ddot{W} - 2m\Omega\dot{U}\sin\beta - m\Omega^2(W\sin^2\beta - V\sin\beta\cos\beta) \qquad (2b)$$

$$M_\zeta' + S_\eta - PV' = J_\zeta(\ddot{V}_b' - \Omega^2 V_b') \qquad (3a)$$

$$M_\zeta' + S_\zeta - PW' = J_\eta(\ddot{W}_b' - \Omega^2 W_b') \quad , \qquad (3b)$$

where J is the rotatory inertia.

Generally, the lowest axial frequency is greater than ten times the rotor speed, so we shall ignore the axial motion and its derivatives. The CF resultant P is assumed to be independent of time and is found by simple integration. These assumptions on the U-motion cause the Coriolis terms to be eliminated.

As the axial stiffness EA is usually large, U << 1 and can be ignored in (1). Hence the resultant for axial force is obtained by simple integration,

$$P(x) = \frac{1}{2} m\Omega^2(\ell^2 - x^2) \quad . \qquad (4)$$

Since the total lateral displacement is the sum of shear and bending components, the moment-curvature and shear relations for a Timoshenko beam become [7]:

$$M_\zeta = EI_\zeta V_b'' \quad , \quad V_s' = \frac{1}{Gk_\eta A}(S_\eta - PV') \qquad (5a)$$

$$M_\eta = EI_\eta W_b'' \quad , \quad W_s' = \frac{1}{Gk_\zeta A}(S_\zeta - PW') \qquad (5b)$$

Substituting (5a), (5b) into (2a) and (3a), (2b) and (3b) respectively, the usual algebraic manipulations lead to the equations of motion in terms of total deflections:

$$EI_\zeta V'''' + m\left[\ddot{V} - \Omega^2(V\cos^2\beta - W\sin\beta\cos\beta)\right] - (PV')' - \frac{EI_\zeta}{Gk_\eta A}\left[m\ddot{V}'' - m\Omega^2(V''\cos^2\beta - W''\sin\beta\cos\beta) - (PV')'''\right] - J_\zeta(\ddot{V} - \Omega^2 V)'' - \frac{J_\zeta}{Gk_\eta A}\left\{m(\ddot{V}'' - \Omega^2\ddot{V}) - \left(P(\ddot{V} - \Omega^2 V)'\right)' - m\Omega^2\left[\cos^2\beta(\ddot{V} - \Omega^2 V) - \sin\beta\cos\beta(\ddot{W} - \Omega^2 W)\right]\right\} = 0$$

$$EI_\eta W'''' + m\left[\ddot{W} - \Omega^2(W\sin^2\beta - V\sin\beta\cos\beta)\right] - (PW')' - \frac{EI_\eta}{Gk_\zeta A}\left[m\ddot{W}'' - m\Omega^2(W''\sin^2\beta - V''\sin\beta\cos\beta) - (PW')'''\right] - J_\eta(\ddot{W} - \Omega^2 W)'' - \frac{J_\eta}{Gk_\zeta A}\left\{m(\ddot{W}'' - \Omega^2\ddot{W}) - \left(P(\ddot{W} - \Omega^2 W)'\right)' - m\Omega^2\left[\sin^2\beta(\ddot{W} - \Omega^2 W) - \sin\beta\cos\beta(\ddot{V} - \Omega^2 V)\right]\right\} = 0$$

. . . (6)

The motion is assumed to be steady and harmonic, hence a set of ordinary differential equations is obtained by introducing:

$$\begin{bmatrix} V(x,t) \\ W(x,t) \end{bmatrix} = \begin{bmatrix} v(x,t) \\ w(x,t) \end{bmatrix} e^{i\omega t} \qquad (7)$$

where ω is the natural frequency. It is also convenient to use the following non-dimensional coefficients:

$$\alpha = m\ell^4\Omega^2/EI \quad \text{(angular speed)} \quad , \quad \lambda = m\ell^4\omega^2/EI \quad \text{(frequency)} \qquad (8)$$

$$\delta = EI/GkA\ell^2 \quad , \quad \varepsilon = J/m\ell^2 \quad \text{(shear deflection and rotatory inertia coefficients)}$$

where subscripts η and ζ will indicate that the appropriate cross-sectional constants are used. The quantities δ and ε are small for practical geometries.

Substitution of (7) and (8) into (6) yields a pair of fourth order variable coefficient ordinary differential equations for the mode shape. For lead-lag motion,

$$(1 + \delta\alpha p)v'''' + 3\alpha\delta pv''' - \left[1 - \varepsilon\delta(\lambda + \alpha)\right]\left[(\lambda + \alpha\cos^2\beta)v + \alpha p'v' - \underline{\alpha w\cos\beta\,\sin\beta}\right]$$

$$+ \left[\varepsilon(\lambda + \alpha)(1 + \delta\alpha p) + \delta(\lambda + \alpha\cos^2\beta) - \alpha(p - 3\delta p'')\right]v'' - \underline{\delta\alpha w''\cos\beta\,\sin\beta} = 0 \qquad . . (9a)$$

where subscript η is implied on parameters α, λ, δ and ε. For flapping motion,

$$(1 + \delta\alpha p)w'''' + 3\alpha\delta pw''' - \left[1 - \varepsilon\delta(\lambda + \alpha)\right]\left[(\lambda + \alpha\sin^2\beta)w + \alpha p'w' - \underline{\alpha v\cos\beta\,\sin\beta}\right]$$

$$+ \left[\varepsilon(\lambda + \alpha)(1 + \delta\alpha p) + \delta(\lambda + \alpha\sin^2\beta) - \alpha(p - 3\delta p'')\right]w'' - \underline{\alpha\delta v''\cos\beta\,\sin\beta} = 0 \qquad . . (9b)$$

where subscript ζ is implied. The primes denote differentiation with respect to the non-dimensional coordinate $\xi = x/\ell$.

Coupling between v and w motions is introduced through the non-conservative CF terms and is represented by the terms underlined. The general solution of (9) requires the solution of an eighth order equation. Under certain assumptions, the two fourth-order equations decouple and independent solutions for flapping and lead-lag are obtained.

3. UNTWISTED BEAMS AT ZERO INCIDENCE

For an untwisted beam at zero incidence ($\beta \equiv 0$), axes (η,ζ) and (x,y) coincide and decouple. Hence for lead-lag

$$(1 + \delta\alpha p)v'''' + 3\delta\alpha pv''' - \left[1 - \varepsilon\delta(\lambda + \alpha)\right]\left[\alpha p'v' + (\lambda + \alpha)v\right]$$

$$+ \left[(\varepsilon + \delta + \varepsilon\delta\alpha p)(\lambda + \alpha) - \alpha(p - 3\delta p'')\right]v'' = 0 \qquad (10)$$

where subscript $\eta \equiv y$ is implied for the physical parameters. The flapping equation (with implied subscript $\zeta \equiv z$) becomes

$$(1 + \delta\alpha p)w'''' + 3\delta\alpha pw''' - \left[1 - \varepsilon\delta(\lambda + \alpha)\right](\alpha p'w' + \lambda w)$$

$$+ \left[\delta\lambda + (\varepsilon + \varepsilon\delta\alpha p)(\lambda + \alpha) - \alpha(p - 3\delta p'')\right]w'' = 0 \qquad (11)$$

Care must be taken with the boundary conditions, for often only the bending component of slope can be specified at a boundary. Combining (2) and (5) the bending slopes can be obtained in terms of total displacements,

$$v_b' = \frac{\delta(1 + \alpha\delta p)v''' + 2\alpha\delta^2 p'v'' + \left[1 + \delta^2(\lambda + \alpha + \alpha p'')\right]v'}{\ell\left[1 - \varepsilon\delta(\lambda + \alpha)\right]} \qquad (12)$$

$$w_b' = \frac{\delta(1 + \delta\alpha p)w''' + 2\delta^2\alpha p'w'' + \left[1 + \delta^2(\lambda + \alpha p'')\right]w'}{\ell\left[1 - \varepsilon\delta(\lambda + \alpha)\right]} \qquad (13)$$

Differentiating the second of (5) and using (2) and (3), the moments can be obtained in terms of total displacements:

$$M_z = \frac{EI_z}{\ell^2}\left[(1 + \alpha\delta p)v'' + \alpha\delta p'v' + \delta(\lambda + \alpha)v\right] \tag{14}$$

$$M_y = \frac{EI_y}{\ell^2}\left[(1 + \delta\alpha p)w'' + \delta\alpha p'w' + \delta\lambda w\right] \tag{15}$$

Similarly, the shear force is obtained from (3):

$$S_y = \frac{-EI_z\left\{(1 + \delta\alpha p)v''' + 2\delta\alpha p'v'' + \left[(\varepsilon + \delta + \varepsilon\delta\alpha p)(\lambda + \alpha) - \alpha(p - \delta p'')\right]v'\right\}}{\ell^3\left[1 - \varepsilon\delta(\lambda + \alpha)\right]} \tag{16}$$

$$S_z = \frac{-EI_y\left\{(1 + \delta\alpha p)w''' + 2\delta\alpha p'w'' + \left[\delta\lambda + (\varepsilon + \varepsilon\delta\alpha p)(\lambda + \alpha) - \alpha(p - \delta p'')\right]w'\right\}}{\ell^3\left[1 - \varepsilon\delta(\lambda + \alpha)\right]} \tag{17}$$

Note that in the pairs (12) - (13), (14) - (15), and (16) - (17), the physical parameters have the subscripts η and ζ respectively, e.g. α_η, α_ζ, λ_η, λ_ζ, etc.

4. POWER SERIES SOLUTIONS

Since equations (10 and (11) are linear real ordinary differential equations, the solution can be expressed in terms of real positive integer powers of the dependent variable. Thus the solution is assumed in the form

$$X(\xi) = \sum_{n=0}^{\infty} A_n \xi^n \tag{18}$$

where the dependent variable may be $v(\xi)$ or $w(\xi)$. It is necessary to write the axial force as

$$p(\xi) = a + b\xi + c\xi^2 \tag{19}$$

For discontinuous beams, or beams with concentrated masses, constants a,b and c will also be discontinuous.

After substitution of (18) and (19) into (10), coefficients of like powers of ξ are collected and the following recurrence formula is obtained for lead-lag motion,

$$\begin{aligned}(1 + \alpha\delta a)A_{n+4} = &-\frac{\alpha\delta b(n+3)A_{n+3}}{n+4} \\ &- \left\{\delta(\lambda+\alpha) - \alpha a + \varepsilon(\lambda+\alpha)(1 + \alpha\delta a) + (n+3)(n+2)\alpha\delta c\right\}\frac{A_{n+2}}{(n+4)(n+3)} \\ &+ \left[1 - \varepsilon\delta(\lambda+\alpha)\right]\frac{(n+1)^2\alpha b\, A_{n+1} + \left[\lambda + \alpha + n(n+1)\alpha c\right]A_n}{(n+4)(n+3)(n+2)(n+1)}, \quad n \geq 0 .\end{aligned} \tag{20}$$

Substitution of (18) and (19) into (11) yields a similar equation for flapping

which is obtained from (20) by deletion of the terms with bold underlines.

Inspection of (20) shows that only four coefficients can be chosen arbitrarily and these are taken to be A_0 through A_3. Hence four independent functions are defined as follows:

$$\begin{aligned} F_1(\xi) &= 1 + A_4^1 \xi^4 + A_6^1 \xi^6 + A_8^1 \xi^8 + \ldots , \\ F_2(\xi) &= \xi + A_5^2 \xi^5 + A_7^2 \xi^7 + A_9^2 \xi^9 + \ldots , \\ F_3(\xi) &= \xi^2 + A_4^3 \xi^4 + A_6^3 \xi^6 + A_8^3 \xi^8 + \ldots , \\ F_4(\xi) &= \xi^3 + A_5^4 \xi^5 + A_7^4 \xi^7 + A_9^4 \xi^9 + \ldots , \end{aligned} \tag{21}$$

The coefficients are all obtained from (20) by using the following initial values:

$$\text{For } F_i(\xi) \text{ , set } \begin{cases} A_k^i = 0, \; k = 0, 1, 2, 3 \text{ and} \\ A_{i-1}^i = 1 \end{cases} \tag{22}$$

For example, to generate F_3, set $A_0^3 = A_1^3 = A_3^3 = 0$ and $A_2^3 = 1$. Then (20) is used to generate the remaining terms*.

The general solution of (10) or (11) can now be written as

$$v(\xi) = C_1 F_1(\xi) + C_2 F_2(\xi) + C_3 F_3(\xi) + C_4 F_4(\xi) , \tag{23}$$

where constants C_i are determined from four boundary conditions at the ends.

In the degenerate case of no rotation and zero rotatory inertia and shear deformation ($\delta = \varepsilon = \alpha = 0$), the recurrence formula reduces to

$$A_{n+4} = \frac{\lambda A_n}{(n+1)(n+2)(n+3)(n+4)} , \quad \lambda = (\beta \ell)^4 , \tag{24}$$

and the usual Timoshenko beam functions (Ref. 8, p.338) are recovered.

5. PROGRAMMING CONSIDERATIONS

Beam functions $F_i(\xi)$ and their derivatives can be treated as known functions by constructing a FORTRAN function sub-program of (21) using (22) and (20). For a simple cantilever, deflection and slope are equated to zero at the clamp as are moment and shear at the free end. The result is four simultaneous homogeneous equations, and for constants C_i to be non-zero the determinant must vanish. Hence a simple interval halving method is used to search a pre-defined range for the discrete real values λ_i which give a zero determinant. The actual natural frequency ω_i is then obtained from (8).

Actual rotor blades are seldom uniform, and often consist of a root segment followed by a relatively uniform blade having perhaps one or more balance weights. In most cases this can be idealized as an assembly of n segments, resulting in a 4n x 4n determinant. When the determinant becomes large, the value near a root also remains large, e.g. 10 exp 30 for one 12 x 12. Hence it is convenient both numerically and formally to employ a transfer matrix method (our notation is similar to that of Pestel & Leckie {2}). By placing

---

* The superscripts on A_n were introduced to denote that the coefficients for each function are independently generated. Thus $A_4^1 \neq A_4^3$, $A_7^2 \neq A_7^4$, etc.

deflection, bending slope, moment and shear in a column vector (usually termed a state vector), they can be related to the undetermined constants C_i by a 4 x 4 matrix $\underset{\sim}{B}$,

$$\underset{\sim}{z}(\xi) = \underset{\sim}{B}(\xi)\,\underset{\sim}{a}\ , \qquad \underset{\sim}{z} = \{v\ ,\ v_b'\ ,\ M\ ,\ S\}\ ,\quad \underset{\sim}{a} = \{C_1\ ,\ C_2\ ,\ C_3\ ,\ C_4\} \tag{25}$$

The individual terms in $\underset{\sim}{B}$ are (21) and (10) through (17),

$$\begin{aligned} B_{1,j} &= F_j(\xi) \ , & B_{2,j} &= v_b'\left[v = F_j(\xi)\right] \\ B_{3,j} &= M\left[v = F_j(\xi)\right] \ , & B_{4,j} &= S\left[v = F_j(\xi)\right] \end{aligned} \tag{26}$$

The notation $\left[v = F_j(\xi)\right]$ denotes that throughout the expression $v(\xi)$ and its derivatives are replaced by $F_j(\xi)$.

Consider a beam composed of n segments as shown in Fig. 3.

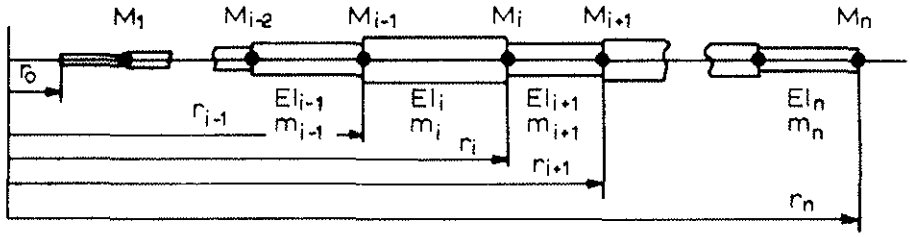

FIG. 3: Generalized rotating beam.

If $\underset{\sim}{z}_i(0)$ and $\underset{\sim}{z}_i(1)$ are the state vectors at the beginning and end of the i-th segment, then

$$\underset{\sim}{z}_i(1) = \underset{\sim}{B}_i(1)\cdot\underset{\sim}{B}_i^{-1}(0)\cdot\underset{\sim}{z}_i(0) = \underset{\sim}{U}_i\underset{\sim}{z}_i(0)\ , \tag{27}$$

where $\underset{\sim}{U}_i$ is the transfer matrix for the i-th segment. A concentrated mass may be included at the interface between two segments as shown in Fig. 3, and the transfer matrix from segment i to segment i+1 for the lead-lag motion is

$$\underset{\sim}{z}_{i+1}(0) = \underset{\sim}{P}_i\,\underset{\sim}{z}_i(1)\ , \quad \underset{\sim}{P}_i = \begin{bmatrix} 1 & 0 & C & 0 \\ 0 & 1 & 0 & 0 \\ 0 & 0 & 1 & 0 \\ -\underline{M_i(\Omega^2+\omega^2)} & 0 & 0 & 1 \end{bmatrix} \tag{28}$$

For flapping motion the underlined term is deleted. Hence the state vector at any point can be expressed in terms of the root or initial vector $z_i(0)$; at the tip,

$$\underset{\sim}{z}_n(1) = \underset{\sim}{D}\,\underset{\sim}{z}_1(0)\ , \quad \underset{\sim}{D} = \prod_{i=1}^{n}\underset{\sim}{P}_i\,\underset{\sim}{U}_i \tag{29}$$

The boundary conditions are now imposed and (29) is partitioned in displacement and force parts. For a cantilevered blade,

$$\begin{matrix} d_n \\ 0 \end{matrix} = \begin{bmatrix} D_{dd} & D_{df} \\ D_{fd} & D_{ff} \end{bmatrix} \cdot \begin{bmatrix} 0 \\ f_0 \end{bmatrix} \qquad \begin{aligned} d_n &= \{ v_n(1) \ , \ v_{b_n}'(1) \} \\ f_0 &= \{ M_1(0) \ , \ S_1(0) \} \end{aligned} \tag{30}$$

The second of (30) yields the frequency determinant $| D_{ff} | = 0$, and the mode shape is obtained from (30), (29), (27) and (25) in the usual way.

Care must be taken that the CF is properly represented. For the i-th segment,

$$\begin{aligned} p(\xi) &= a_i + b_i\xi + c_i\xi^2 \quad , \quad 0 \le \xi \le 1 \quad , \\ a_i &= \frac{1}{m_i \ell_i} \sum_{j=i}^{n} m_j \ell_j \ (r_j - \ell_j/2) + M_j r_j \\ b_i &= (1 - r_i/\ell_i) \ , \quad c_i = -1/2 \ , \ \ell_i = r_i - r_{i-1} \end{aligned} \tag{31}$$

Coefficients (8) may also vary from segment to segment, and overall convergence was improved when segment length $\ell_i = r_i - r_{i-1}$ was used in (8).

A variety of FORTRAN programs can be readily constructed using (26) to build (29) and (30), and results for test values and a typical helicopter rigid rotor blade are illustrated.

6. TWISTED NON-UNIFORM BEAMS

There are a variety of rotating beams like propeller and turbine blades which are difficult to model with the preceding straight beam formulae. The previous techniques can be readily extended to non-uniform twisted beams by subdividing the beam into piecewise uniform segments. Each segment may have an arbitrary angle of incidence β as shown in Fig. 4.

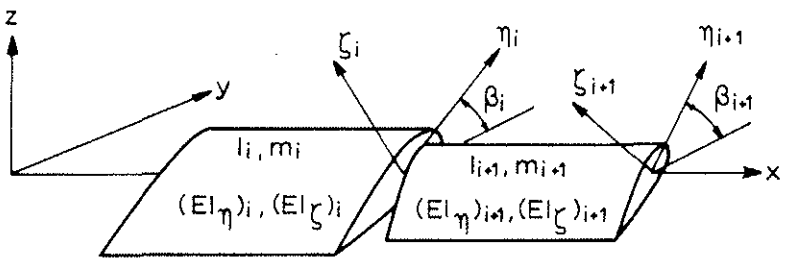

FIG. 4: Idealization of a twisted non-uniform beam.

Rotatory inertia and shear deflections are not included here, since for most propeller and turbine problems only 1st and 2nd mode frequencies are required, for which the Timoshenko corrections will be small, as shown in Section 7. Thus, equations (9) reduce to:

$$\begin{aligned} v'''' - (\alpha_\eta \cos^2\beta + \lambda_\eta)v - \alpha_\eta (Pv')' + \alpha_\eta \cos\beta \ \sin\beta w &= 0 \\ w'''' - (\alpha_\zeta \sin^2\beta + \lambda_\zeta)w - \alpha_\zeta (Pw')' + \alpha_\zeta \cos\beta \ \sin\beta v &= 0 \end{aligned} \tag{32}$$

Coupling between flapping and lead-lag is introduced through the non-conservative CF terms and is represented by the last term in each of (32). The general solution of (32) would require an infinite series solution for an eighth order equation. However an approximate pair of fourth order equations

were obtained by ignoring the coupling term in (32). The significance of this approximation will be discussed at the end of this section where its effect will be apparent.

Equations (32) less the coupling terms were solved via the Frobenius method as in Section 4. Using (19) to express the axial force, the recursion formulae for lead-lag and flapping become

$$(n+3)(n+4)A_{n+4} = \left(\frac{\alpha_\eta \cos^2\beta + \lambda_\eta}{n+1} + \alpha_\eta - cn \right) \frac{A_n}{n+2} + \frac{\alpha_\eta b(n+1)A_{n+1}}{n+2} + \alpha_\eta a A_{n+2} \quad ,$$

$$(n+3)(n+4)A_{n+4} = \left(\frac{\alpha_\zeta \sin^2\beta + \lambda_\zeta}{n+1} + \alpha_\zeta - cn \right) \frac{A_n}{n+2} + \frac{\alpha_\zeta b(n+1)A_{n+1}}{n+2} + \alpha_\zeta a A_{n+2} \quad . \qquad (33)$$

Equations (21) through (23) for the mode shapes v and w apply here without change.

The method of transfer matrices outline in Section 5 is also useful here. To account for the coupling of lead-lag and flapping in twisted blades, both must be included in the state vector,

$$\begin{aligned} \underset{\sim}{z}(\xi) &= \underset{\sim}{B}(\xi)\, \underset{\sim}{a} \quad , \\ \underset{\sim}{a} &= \{C_{1\eta}, C_{1\zeta}, C_{2\eta}, C_{2\zeta}, C_{3\eta}, C_{3\zeta}, C_{4\eta}, C_{4\zeta}\} \quad , \\ \underset{\sim}{z} &= \{v, w, v', w', M_\eta, M_\zeta, S_\eta, S_\zeta\} \quad , \end{aligned} \qquad (34)$$

where B is an 8 x 8 matrix formed in a way similar to (26). The 8 x 8 transfer matrix for the i-th element is identical in form to (27). An equation for point masses (balance weights) was not included here as these are rarely used on propellers.

Segment i is connected to segment i + 1 by transforming $\underset{\sim}{z}_i(1)$ to the local coordinates of segment i + 1 ,

$$\begin{aligned} \underset{\sim}{z}_{i+1}(0) &= \underset{\sim}{T}_i\, \underset{\sim}{z}_i(1) \quad , \quad \underset{\sim}{T}_i = \left[\underset{\sim}{R}_i , \underset{\sim}{R}_i , \underset{\sim}{R}_i , \underset{\sim}{R}_i \right] \quad , \\ \underset{\sim}{R}_i &= \begin{bmatrix} \cos\Delta\beta_i , & \sin\Delta\beta_i \\ -\sin\Delta\beta_i , & \cos\Delta\beta_i \end{bmatrix} , \quad \Delta\beta_i = \beta_{i+1} - \beta_i \quad . \end{aligned} \qquad (35)$$

Hence the state vector at the tip can be expressed in terms of the root vector by

$$\underset{\sim}{z}_n(1) = \underset{\sim}{P}\, \underset{\sim}{z}_1(0) \quad , \quad \underset{\sim}{D} = \prod_{i=1}^{n} (T_i \cdot U_i) \qquad (36)$$

The boundary conditions reduce the 8 x 8 matrix to a fully populated 4 x 4 frequency determinant, and the FORTRAN program VGBLADE for frequency analysis of propeller blades is given in Ref. {9}.

For a single segment blade with $\Omega^2 >> \omega^2$, the deletion of the coupling terms in (32) would cause a serious error of several per cent. However, the subdivision of a blade into several segments (10 for a typical propeller) mitigates this error. The term $\cos\beta(\alpha_\eta w \sin\beta)$ from the first of (32) is partially recovered at each segment boundary as the rotation matrix T effectively includes this in the second terms of (32). Thus, to first order, only the variation of the coupling term over each segment has been ignored. Most applications will require several segments to represent the variation of incidence and section properties, and the decoupling approximation should not introduce errors more serious than the deletion of the Timoshenko corrections.

7. RESULTS OF TESTS AND APPLICATIONS

The theory outlined in the previous sections was used to analyse a variety of representative problems of blade bending vibrations. The computer programs LEADLAG, FLAP, and VGBLADE were developed for the above analysis and are available with Ref. {9} from the authors.

7.1 Comparison with Tests

The effect of rotation speed was tested for uniform cantilevers fixed on a rotating hub. Here the merits of the present method are highlighted since the beam-function solution to the exact differential equations allows the rotating uniform beams to be tackled with only one segment. The results are compared graphically with those obtained by Carnegie {10} which include tests and an approximate analysis. Fig. 5 shows the variation of the first 4 bending frequencies with rotation speed; the improvement due to the present analysis is quite definite, especially for the higher modes and at the higher rotation speeds.

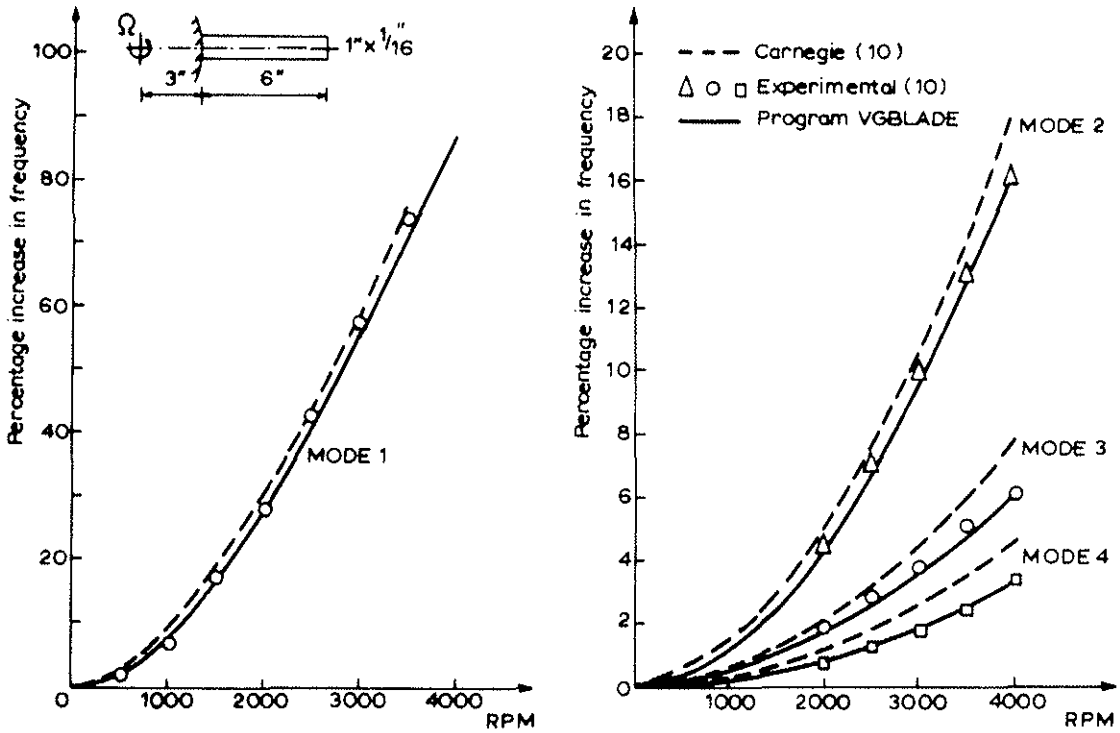

FIG.5: Variation of natural frequency with rotation speed.

7.2 A Helicopter Rigid Rotor

To test its general applicability the helicopter main rotor blade shown in Fig. 6 was analysed; the values shown are similar to actual blades. The first test was to generate the classic spoke diagram, and two segments were used to represent the blade without the 1 kg added mass. The results for uncoupled lead-lag and flap are shown in Fig. 7. For this blade and its frequency-speed range, the correction to ETB is almost entirely due to the classical term.

The addition of small balancing weights on a blade can shift frequencies considerably. At the operating speed, Fig. 7 shows a potentially dangerous 5Ω

resonance of the second lead-lag mode. Hence two identical segments are used for the aerodynamic portion, their interface being the location of the 1 kg added mass. The position of the 1 kg mass was varied from r = 1 m to the tip, and the resulting mass balancing diagram is shown in Fig. 8.

The first mode frequencies decrease as expected, but the influence of the added mass on the higher modes is more complex. The increase of frequency is due to the added stiffening effect of CF which depends on the relative amplitude of the 1 kg mass. Thus the points of zero frequency change are not node points of the eigenvector, but points where the decrease in ω_i due to added mass is matched by the added CF stiffening. Fig. 8 indicates two preferred positions, point A and the tip; the former would probably be selected for fatigue and other reasons. By using two or more weights, it is possible to shift frequencies nearly independently.

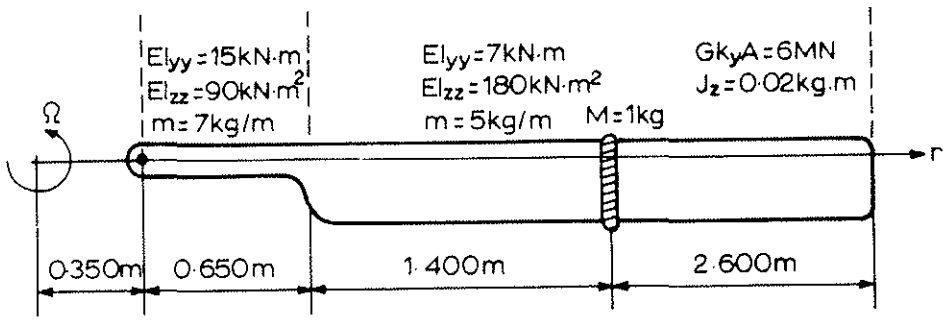

FIG.6: A small helicopter rigid rotor blade

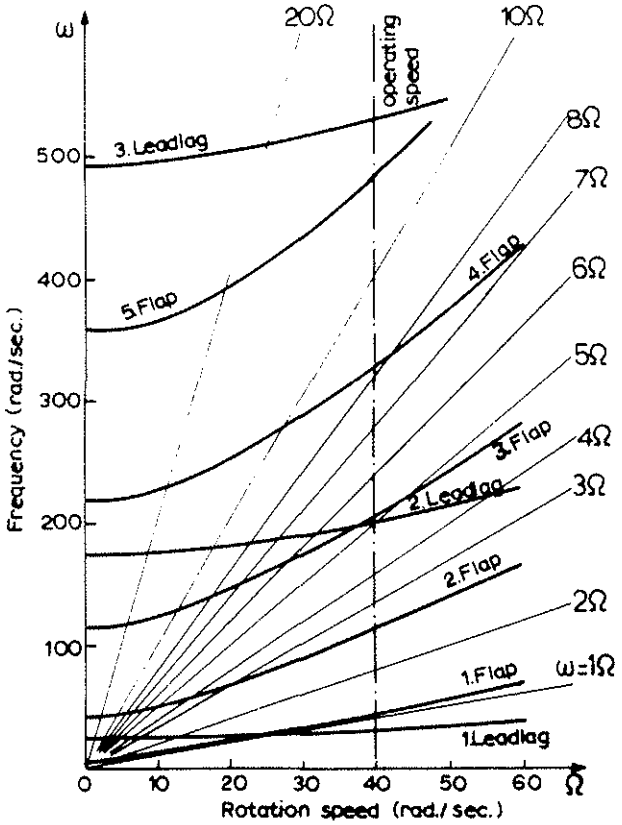

FIG.7: Spoke diagram for a helicopter blade.

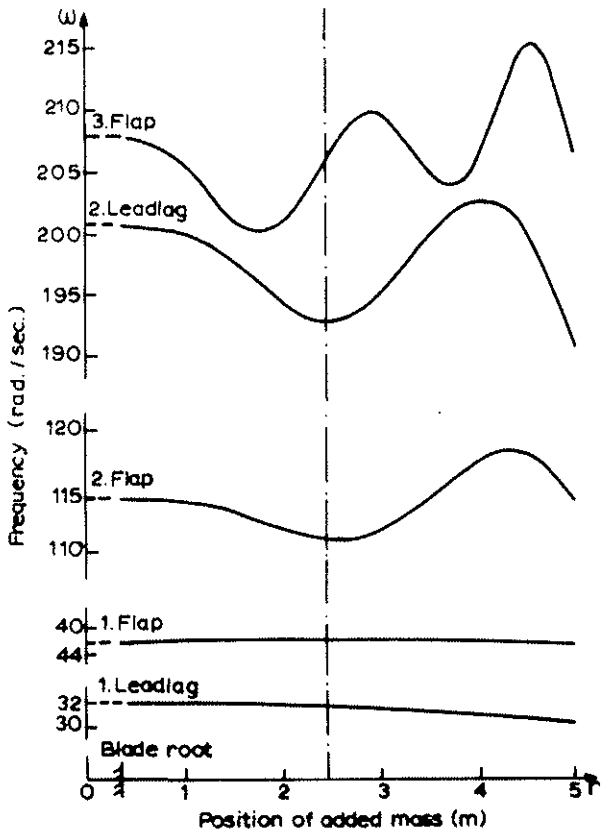

FIG.8: Mass balancing diagram.

7.4 Spoke Diagram for Propeller Blade

High non-uniformity and significant pretwist are the salient features of propeller blades; typical section properties for a medium-size propeller are given in Table 1. Natural frequencies in the range 0-1500 rad/sec were determined for rotating speeds of 0-500 rad/sec.

Since different search procedures are preferred by various designers, the program gives the option of finding the frequencies either at a number of fixed rotation speeds, or along a number of Ω-lines. The resulting spoke diagram is presented in Fig. 9. Lead-lag and flap motions cannot be identified as such due to pretwist coupling of the two motions. This leads to features specific to twisted blades, such as the inflection of the second-mode curve.

Radius (in)	Area (in^2)	I_{min} (in^4)	I_{max} (in^4)	Twist (β^o)
14.50	18	9.00	85	35
21.75	16	5.00	95	27
29.00	13	2.50	97	19
36.25	11	1.00	92	12
43.50	9	.60	91	8
50.75	8	.40	85	4
58.00	7	.30	74	0
65.25	6	.20	65	-3
72.50	5	.10	54	-6
79.75	4	.05	43	-9
87.00	2	.01	13	-12

Note:

1. $E = 10 \times 10^6$ lbf/in^2, $\rho = .1015$ lb/in^3.
2. Blade angle $\beta_{.7} = 15^o$.

Table 1. Properties of a typical propeller blade

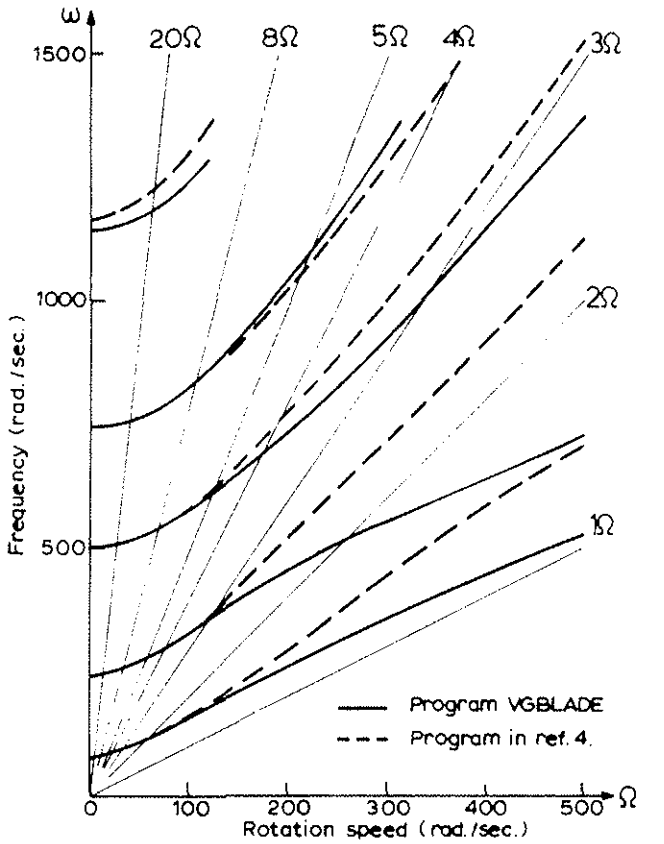

FIG.9: Spoke diagram of typical propeller blade

The same blade was also analysed using the computer program given in Ref. [4], which is based on the Rayleigh-Southwell coefficient. The results are plotted on Fig. 9 for comparison. Though the two methods agree fairly well at low speeds, they diverge significantly at the operating speeds. Since the Rayleigh-Southwell approximation is inherently limited to short, low speed blades, and since it doesn't distinguish between predominantly flap and predominantly lead-lag motions, the disagreement with our exact method is not surprising.

9. CONCLUSIONS

The principal advantage of this semi-analytic method is the exact representation of centrifugal forces, thus its accuracy is independent of the speed of rotation. Although the algebra becomes lengthy, it isn't conceptually difficult and it was relatively simple to include shear deflection and rotatory inertia. In practical applications this approach is attractive for its ease of programming and reliable accuracy over a broad range of parameters. Complete computer programs have been developed for propellers (twisted blades) and helicopter rotor blades, and complete card copies (FORTRAN IV) accompanied with a detailed description/Users manual are available from the authors.

The relative importance of the various corrections depends on several quantities, but for $\delta = 10\varepsilon = 10^{-3}$ (not untypical values), the shear deflection δ accounts for 68% of the total correction, rotatory inertia $J\omega^2$ amounts to 24%, while the extra rotatory inertia term $J\Omega^2$ contributes 8%. However, for $\Omega = 50$ rad/sec, this total correction reduces the fourth frequency by only 3%, hence for many practical applications it appears sufficient to include only the shear deflection term.

For helicopter main rotors and other relatively slow blades where the frequencies greatly exceed the rotational speed, the classical Timoshenko corrections are quite accurate and the usual inclusion of them in rotor programs is entirely justifiable. However, for high speed blades such as some propellers and turbine blades the extra shear deflection terms in rotating beams may dominate the classical Timoshenko terms and yield different (even opposite) corrections.

It was presumed that the beam parameters EI, GkA, and J are available separately. In practice their exact computation is difficult, particularly for GRP and CRP materials, and specific finite element programs for these computations have been developed [11] and reports and publications are in progress.

Although the physical beam considered here is an obvious simplification of real rotor systems having pre-cone and coupled torsion-bending, this analysis appears to be adequate for many practical problems. However, this analysis can be extended to more complex systems, and there is no inherent difficulty with problems such as coupled bending-torsion, or blades with swept tips. Under certain conditions a type of orthogonality of mode shapes can be developed, and a full dynamic analysis is feasible.

REFERENCES

1. G. Isakson and J.G. Eisley, Natural frequencies in bending of twisted rotating and non-rotating beams. NASA TN D-371 (1960).

2. E.C. Pestel and F.A. Leckie, Matrix Methods in Elastomechanics, McGraw-Hill (1973).

3. G. Reichert, Load prediction methods for hingeless rotor helicopters, Specialists Mtng. on Helicopter Rotor Loads Prediction Methods, AGARD-CP-122 (1973).

4. Northern Research and Engineering Corporation, The vibration of blades in axial turbomachinery, Report No. 1088, AD 645156 (1965).

5. A.J. Sobey, Dynamical analysis of the shaft-fixed helicopter blade. R.A.E. TR 73175 (1974).

6. J.C. Houbolt and G.W. Brooks, Differential equations of motion for combined flapwise bending, chordwise bending, and torsion of twisted non-uniform rotor blades. NACA Report 1346 (1958).

7. R.W. Traill-Nash and A.R. Collar, The effects of shear flexibility and rotatory inertia on the bending vibrations of beams. Quart. Journ. Mech. and Applied Maths, 6, 187 (1953).

8. S. Timoshenko, Vibration Problems in Engineering, 2nd Edn. Constable (1937)

9. V. Giurgiutiu and R.O. Stafford, Semi-analytic determination of bending frequencies of propeller and helicopter rotors. I.C. Aero Report 75-02, (1975).

10. W. Carnegie, C. Stirling and J. Fleming, Vibration characteristics of turbine blading under rotation - Results of an initial investigation and details of a high-speed test installation. Proc. Inst. Mech. Engrs. 180, Pt. 31, 124 (1966).

11. M. Pattichis, Coupled bending and torsion of anisotropic cantilevers. M.Sc. Project Report, Aeronautics Department, Imperial College (1974).

ACKNOWLEDGMENT

The authors wish to thank Dowty Rotal Ltd., Dynamic Group. for their assistance with the propellor blade example.